



COLUMBIA UNIVERSITY

Department of Physics



RECENT ELECTROWEAK RESULTS FROM THE CCFR COLLABORATION:
NEUTRINO TRIDENTS AND W-Z INTERFERENCE;
AND THE LORENTZ STRUCTURE OF THE WEAK CURRENT

CCFR Collaboration

NEVIS LABORATORIES

Irvington-on-Hudson, New York

**Recent Electroweak Results from the CCFR Collaboration:
Neutrino Tridents and W-Z Interference;
& the Lorentz Structure of the Weak Current**

Sanjib R. Mishra ¹

Nevis Labs, Columbia University,
Irvington, N.Y., 10533

Representing the CCFR Collaboration:

S.R.Mishra, S.A.Rabinowitz, C.Arroyo, K.T.Bachmann, ²
R.E.Blair, ³ C.Foudas, ⁴ B.J.King, W.C.Lefmann, W.C.Leung,
E.Oltman, ⁵ P.Z.Quintas, F.J.Sciulli, B.G.Seligman, M.H.Shaevitz

Columbia University, New York, NY 10027

F.S.Merritt, M.J.Oreglia, B.A.Schumm⁴

University of Chicago, Chicago, IL 60637

R.H.Bernstein, F. Borcharding, H.E.Fisk, M.J.Lamm,
W.Marsh, K.W.B.Merritt, H.Schellman, D.D.Yovanovitch

Fermilab, Batavia, IL 60510

A.Bodek, H.S.Budd, P. de Barbaro, W.K.Sakumoto

University of Rochester, Rochester, NY 14627

P.H.Sandler, W.H.Smith

University of Wisconsin, Madison, WI, 53706.

**Invited talk presented at the Electroweak Session of
the Moriond Conference at Les Arc, March, 1991.**

¹Address after Aug.1991: Harvard Univ., Cambridge, MA 02138.

²Present address: Widener Univ., Chester, PA 19013.

³Present address: Argonne National Laboratory, Argonne, IL, 60439.

⁴Present address: Univ. of Wisconsin, Madison, WI, 53706.

⁵Present address: LBL, Berkeley, CA 94720.

Abstract: We present two recent electroweak measurements by the CCFR collaboration: **A)** Neutrino tridents, muon pairs induced by neutrino scattering in the Coulomb field of a target nucleus, & **B)** Lorentz structure of the weak current. **A)** : The observed number of tridents after geometric and kinematic corrections, 37.0 ± 12.4 , supports the Standard Model prediction of 45.3 ± 2.3 events. These data provide the first demonstration of the W - Z destructive interference from neutrino tridents, and rule out, at 99% CL, the $V - A$ prediction without the interference. **B)** : Two studies that probe the Lorentz structure of weak current are presented: structure functions from $\bar{\nu}_\mu$ - and ν_μ -induced charged current events; and the inverse muon decay process (IMD), $\nu_\mu + e^- \rightarrow \mu^- + \nu_e$. In the first study, the relative absence of $\bar{\nu}_\mu$ -induced charged current events with respect to ν_μ -induced events at large x (> 0.45) and large y (> 0.70) restricts $|\eta|^2 = |g_R/g_L|^2 < 0.0015$ with 90 % CL (CCFR). Within the framework of left-right symmetric models, this measurement imposes a limit upon the mixing angle of the left and right handed bosons. Unlike the limits imposed by the μ -decay and the nuclear β -decay experiments, the present limit is valid irrespective of the mass of the right handed neutrino. The IMD study enables a complementary limit on the $V + A$ component of the weak current.

A. Neutrino Tridents and W-Z Interference

A neutrino trident is the scattering of a neutrino in the Coulomb field of a target nucleus (N)

$$\nu_\mu(\bar{\nu}_\mu) + N \rightarrow \nu_\mu(\bar{\nu}_\mu) + \mu^+\mu^- + N. \quad (1)$$

Momenta are balanced by the coherent exchange of a virtual photon between one of the emergent muons and the nucleus. The signature is a dimuon event with zero visible hadron energy. In the Standard Model this reaction can proceed via two channels (Fig.A1): charged (W) and neutral (Z) boson exchange. A measurement of this process determines the interference between W and Z channels providing a crucial test of the gauge structure of the Standard Model. We report the first measurement of this destructive interference in ν -tridents.

Many theoretical papers discuss ν -trident production.[A1 – A9] As an almost purely leptonic process, its cross section can be precisely calculated using the known electromagnetic form factor of the iron nucleus. Most early theoretical papers deal only with the $V - A$ theory (W exchange alone) ignoring the $W - Z$ interference. However, in the Standard Model the neutral current channel (Z^0 mode) interferes *destructively* with the charged current channel (W^\pm). Assuming the standard vector and axial-vector couplings, the interference causes an approximate 40% suppression of the trident production as compared to the prediction using W -exchange only.[A8, A9]

In spite of the elegance of the theoretical prediction, the experimental study of ν -tridents has been difficult for two reasons: (a) the extremely small cross section, about 2.3×10^{-5} (4.6×10^{-5}) of the inclusive ν_μ -N ($\bar{\nu}_\mu$ -N) charged current process at $\langle E_\nu \rangle = 160$ GeV; and (b) the relatively low energy of the secondary muon associated with the trident. These difficulties are overcome in a high-statistics high-energy neu-

trino experiment. Early experimental investigations of ν -tridents (for a review, see Ref.[A10]) failed to conclusively demonstrate their existence.[A11, A12, A13] More recently the CCFR experiment[A14], and notably, the CHARM II experiment[A15] have reported clear evidence for ν -tridents. Although these data are consistent with the Standard Model prediction, there has been no demonstration of the destructive interference in this process. In ν_e -e scattering, however, the interference between W and Z exchange has been observed by a LAMPF experiment.[A16]

Neutrino data were accumulated using the Fermilab Tevatron quadrupole triplet neutrino beam (QTB) with the Columbia-Chicago-Fermilab-Rochester (CCFR) detector.[A17] The QTB beam contained muon neutrinos and antineutrinos in the ratio $\simeq \frac{2}{1}$ with usable neutrino energy in the range $10 \leq E_\nu \leq 600$ GeV ($\langle E_\nu \rangle = 160$ GeV). The initial sample of 3.7 million muon triggers were required to have, after fiducial cuts, a muon energy $E_{\mu 1} \geq 9$ GeV ("1" refers to the primary muon). The surviving sample of events with one muon consisted of 1.8×10^6 ν_μ - and 3.6×10^5 $\bar{\nu}_\mu$ -induced events. Dimuon events were extracted from this sample by requiring the presence of a second muon track which passed an energy cut $E_{\mu 2} \geq 4.5$ GeV ("2" refers to the secondary muon).

The initial sample of 3.7 million muon triggers were required to have a transverse event vertex within a square of $2.54m \times 2.54m$ centered in the target calorimeter, a longitudinal vertex at least $4.4m$ upstream of the downstream end of the $16.8m$ long target, and a muon track in the spectrometer. The muon track was required to have an energy $E_{\mu 1} \geq 9$ GeV, and an angle $\theta_{\mu 1} \leq 250$ mrad (where "1" refers to the primary muon). The surviving sample of events with one muon consisted of 1.8×10^6 ν_μ - and 3.6×10^5 $\bar{\nu}_\mu$ -induced events. Dimuon events were extracted from this sample by requiring the presence of a second muon track which passed (1) an energy cut $E_{\mu 2} \geq 4.5$ GeV, and (2) an angle cut $\theta_{\mu 2} \leq 250$ mrad (where "2" refers to the secondary muon).

The efficiency of the dimuon selection was checked with a redundant search using counter pulse heights. The resulting dimuon sample consisted of 8532 events.[A18]

The bulk of the 8532 events are the hadronic dimuon events arising from decays of D , π , and K mesons.[A18] Neutrino trident events were extracted by utilizing the kinematic properties that distinguish them from these hadronic dimuons. First, the two muon invariant mass of a trident is considerably smaller than those due to the hadronic dimuons. We present in Fig.A2 the invariant mass distribution of 8532 data events (solid symbols) and that expected for tridents from a Monte Carlo calculation described below (histogram). Figure A2 indicates that the trident signal region is contained by $M_{\mu\mu} \leq 2$ GeV. Second, since tridents are associated with no hadron energy at the event vertex region (E_{HAD}) in the detector, the signal would appear at $E_{HAD}=0$ (commensurate with the detector E_{HAD} resolution). From a study of background beam muons, which should behave like $E_{HAD}=0$ single-muon events for these purposes, we determined that the detector should measure $E_{HAD} \leq 1$ GeV for more than 80% of the true $E_{HAD}=0$ dimuons.[A17] The trident signal is obtained by simultaneously imposing $M_{\mu\mu} \leq 2$ GeV and $E_{HAD} \leq 1$ GeV cuts. In Fig.A3 we compare the measured E_{HAD} distribution of dimuon data with $M_{\mu\mu} \leq 2$ GeV (circles) with the E_{HAD} distribution of dimuon data with $M_{\mu\mu} > 2$ GeV (crosses). The latter data are normalized to the number of events in the first data set in the region $E_{HAD} > 2$ GeV. We see the clear excess due to tridents in the $E_{HAD} \leq 1$ GeV bin with $M_{\mu\mu} \leq 2$ GeV.

Several points add to the confirmation of the trident signal. First, the measured E_{HAD} distribution is demonstrated to be independent of the invariant mass of the dimuons originating from hadronic sources. Figure A4 shows that the E_{HAD} distribution of the dimuon data with $2 < M_{\mu\mu} \leq 3$ GeV (solid circles) is virtually identical to the E_{HAD} distribution of the dimuon data with $3 < M_{\mu\mu} \leq 5$ GeV (squares). This observation is confirmed by a Monte Carlo study, shown in the inset of Fig.A4, which simulated the hadronic sources of the dimuons. Second, the background contribu-

tion to the trident signal from coherent production of a charged pion,[A19] and its subsequent decay is estimated to be less than 0.30 events. Third, a possible contribution to $E_{HAD}=0$ dimuons from the neutral current diffractive production of J/ψ was eliminated by excluding dimuons with $M_{\mu\mu} = 3.1 \pm 0.4$ GeV.[A20] The invariant mass resolution of our detector is $\approx 8\%$ at the J/ψ peak.

The signal consists of 22 events with measured $E_{HAD} \leq 1$ GeV and $M_{\mu\mu} \leq 2$ GeV with an observed background of 6.4 events calculated from 8 events with $E_{HAD} \leq 1$ GeV and $M_{\mu\mu} > 2$ GeV. The excess of 15.6 events should be corrected for the acceptance of $E_{HAD} < 1$ GeV cut, the geometric reconstruction, the $E_{\mu 1} > 9$ GeV cut, and the $E_{\mu 2} > 4.5$ GeV cut. The efficiency for the last three cuts (which was calculated to be 0.50 for $E_{\mu 2} > 4.5$ GeV cut) was determined from a ν -trident Monte Carlo calculation discussed below. The Monte Carlo indicates, and data confirm, that the most sensitive cut is that on $E_{\mu 2}$. We therefore repeated the analysis with an $E_{\mu 2}$ cut at 5 GeV and at 9 GeV. The results, enumerated in Table A1, show that our extraction of this signal is independent of the choice of $E_{\mu 2}$ cut. We report a trident signal, after all corrections, of

$$N(\text{Data}) = 37.0 \pm 12.4. \quad (2)$$

To confront the theoretical prediction and calculate efficiencies, trident production was simulated using the exact calculation by K.Fujikawa.[A4]. The trident matrix element calculation of the Feynman diagram in Fig.A1 was explicitly checked against the exact calculations due to W.Czyz *et al.*,[A2], and R.W.Brown *et al.*[A7] These agreed within 3%; and were also in agreement with the approximate calculation (using a virtual photon approximation) in Refs.[A1,A9]. The iron nucleus electromagnetic form factor was taken from the electron scattering data.[A21] The contribution to the trident signal from incoherent scattering from target *nucleons* (as opposed to scattering off target *nuclei*), was also included, where the nucleon

form factor was taken from Olsson *et al.*[A22] Target nucleons contribute approximately 1/5 of the tridents produced by target nuclei.[A23] It should be noted that the trident calculation is rather precise; the form factors measurements do not constitute the largest source of error. The largest source of theoretical uncertainty is the estimation of the Pauli suppression which affects only the neutrino-nucleon trident production (16% of the total trident production cross section). The combined systematic error on the theoretical prediction of ν -tridents is estimated to be 5%. For W -exchange alone, or for the $V - A$ theory, the predicted number of trident events is:

$$N(\text{Trident: V-A}) = 78.1 \pm 3.9. \quad (3)$$

The prediction of the Standard Model including both W and Z exchange, is:

$$N(\text{Trident: Standard Model}) = 45.3 \pm 2.3 \quad (4)$$

Our data, with 37.0 ± 12.4 events, clearly support the destructive interference hypothesis; and rules out the lack of interference at $> 99\%$ CL.

The trident cross section can be calculated from the measured absolute ν - N charged current cross section of,[A17] $\sigma_{\nu N}(\text{CC}) = (0.680 \pm 0.015)E_\nu \times 10^{-38} \text{ cm}^2/\text{GeV}$, and the observed rate of tridents with respect to all charged current interactions (rate = $(1.33 \pm 0.43) \times 10^{-5}$). The cross section is:

$$\sigma(\nu \text{ Trident}) = (4.7 \pm 1.6)E_\nu \times 10^{-42} \frac{\text{cm}^2}{\text{Fe Nucleus}} \text{ at } \langle E_\nu \rangle = 160 \text{ GeV}. \quad (5)$$

B: Lorentz Structure of Weak Current in ν Interactions and Inverse Muon Decay

Ever since the discovery of parity violation, and, indeed, the realization that the weak current violates parity *maximally*, there has been a relentless quest for a small but non-zero component of parity conserving weak interaction. A natural laboratory to discern a finite $V + A$ component of the weak interaction is collating the differential cross section of $\bar{\nu}_\mu$ -N charged current events (CC) with those of ν -induced events. A departure from the characteristic y -dependence will signal a space-time structure of the weak current different from the assumed $V - A$. Precision measurements of parameters in μ -decay and in nuclear β -decay impose stringent constraints on right handed currents *coupled to light neutrinos*. Neutrino measurements, on the other hand, are *independent of neutrino mass assumptions*; and with the recent limits on $V + A$ currents set by the CCFR collaboration are now competitive with the limits from the low energy domain.

Neutrino interactions exhibit, via their y dependence, the helicity of the weak current. If there were a right handed coupling, the ν_μ -N and $\bar{\nu}_\mu$ -N differential cross sections would assume forms:

$$\begin{aligned} \frac{d\sigma^\nu}{dx dy} &= \frac{G^2 M x E_\nu}{\pi} \left[(q(x) + (1-y)^2 \bar{q}(x)) + \eta^2 (\bar{q}(x) + (1-y)^2 q(x)) \right] \quad --(a) \\ \frac{d\sigma^{\bar{\nu}}}{dx dy} &= \frac{G^2 M x E_\nu}{\pi} \left[(\bar{q}(x) + (1-y)^2 q(x)) + \eta^2 (q(x) + (1-y)^2 \bar{q}(x)) \right] \quad --(b), \quad (6) \end{aligned}$$

where the parameter $|\eta| = |g_R/g_L|$ signifies the relative coupling of the right and the left handed currents. We assume a left handed neutrino, created in π/K decay, interacting via a $V - A$ current at the lepton vertex; the right handed coupling evinces at the quark vertex (see below). Theories with manifest left-right symmetry make definite prediction about η within the context of ν -N scattering.[B1] In such theories with an enlarged gauge group, $SU(2)_L \times SU(2)_R \times U(1)$, the left (W_L) and

right (W_R) handed bosons mix:

$$\begin{aligned} W_1 &= W_L \cos \zeta + W_R \sin \zeta \\ W_2 &= -W_L \sin \zeta + W_R \cos \zeta. \end{aligned} \quad (7)$$

The left handed currents couple predominantly to W_1 and right handed to W_2 . The left (g_L) and the right (g_R) handed coupling in these models are, $g_L = (\cos^2 \zeta)/M_1^2 + (\sin^2 \zeta)/M_2^2$ and $g_R = (\sin \zeta \cos \zeta)(1/M_1^2 - 1/M_2^2)$. The parameter η , whose non-zero value would indicate the existence of right handed coupling, is then expressed as: $|\eta| = |g_R/g_L| = \zeta(1 - M_1^2/M_2^2) = \zeta(1 - \epsilon)$. (We have followed the symbolic notation due to Strovink[B2]).

The parameter η is measured by forming appropriate ratio of two structure functions: $q_L(x) = q(x) + \eta^2 \bar{q}(x)$, and $q_R(x) = \bar{q}(x) + \eta^2 q(x)$ in equation (6). The structure functions, q_L and q_R , are extracted by using the y -dependence of the above two differential cross sections. For large values of y , where the terms of the order $(1 - y)^4$ become negligible, $q_R(x)$ can be expressed as:

$$q_R(x) \propto \frac{d\sigma^{\bar{\nu}}}{dx dy} - (1 - y)^2 \frac{d\sigma^{\nu}}{dx dy}. \quad (8)$$

Experimentally, for large values of x , $q_R(x) \ll q_L(x)$. This imposes an upper limit on the sum $\bar{q}(x) + \eta^2 q(x)$. Limits on the right handed coupling in ν -N interactions have been obtained by the CDHS collaboration[B3] and, later, in a similar analysis with higher statistics at higher neutrino energy and mean Q^2 by the CCFR collaboration.[B4]

Three experimental graphs (Fig's B1a, B1b, and B2), obviate the need for a $\eta^2 > 0$, within the accuracy of the CCFR data. In Fig.B1a (Fig.B1b) the observed ν_μ -induced ($\bar{\nu}_\mu$ -induced) y -distribution is shown, and is compared to a Monte Carlo

prediction. (The Monte Carlo assumes a $V - A$ current coupling with quark and antiquark distributions iteratively extracted from the data). In Fig.B2, $\bar{q}(x, Q^2) \approx .5 \times [F_2(x, Q^2) - xF_3(x, Q^2)]$ in various x -bins is shown. The good agreement between the data and the Monte carlo y -distributions (Fig's B1a and B1b), and the fact that $\bar{q}(x)$ is consistent with zero for $x \geq 0.45$ (Fig.B2) indicates an $|\eta|^2$ consistent with zero. Stated differently, these figures indicate that the ratio of ratio of antineutrino to neutrino cross sections at large and small values of x , $\left[\frac{d\sigma^{\bar{\nu}}}{dy} / \frac{d\sigma^{\nu}}{dy} \right]_{x>.45} / \left[\frac{d\sigma^{\bar{\nu}}}{dy} / \frac{d\sigma^{\nu}}{dy} \right]_{x<.10}$, is extremely small for large values of y . This observed small ratio, then, enables one to limit $|\eta|^2$.

To measure η^2 , CC data with large x and y are selected. We impose a cut $x > 0.45$ and $y > 0.70$; the average energy and Q^2 of surviving events are 208 GeV and 170 GeV² respectively. The upper limit on $|\eta|^2$ is obtained by extracting an upper limit on,

$$\left[\frac{d\sigma^{\bar{\nu}}}{dx dy} - (1 - y)^2 \frac{d\sigma^{\nu}}{dx dy} \right] / \left[\frac{d\sigma^{\nu}}{dx dy} - (1 - y)^2 \frac{d\sigma^{\bar{\nu}}}{dx dy} \right]. \quad (9)$$

Corrections due to geometric acceptance and resolution smearing are applied to the data using a Monte Carlo. In addition model corrections due to radiative, iso-scalar, charm quark threshold, and propagator effects are incorporated. The effect of a non-zero R (σ_L/σ_T), neglected in equation 6 for clarity, was estimated in Monte Carlo studies using the alternative parametrization of R_{QCD} , R_{QCD} with target mass effects, and R_{SLAC} . [B5] The systematic uncertainties associated in the $|\eta|^2$ measurement are detailed in Table B1. The CCFR measurement yields a limit for $|\eta|^2$:

$$|\eta|^2(x < 0.45, y > 0.70) < 0.0015(90\% \text{ CL}). \quad (10)$$

The limit by the CDHS collaboration is $|\eta|^2 < 0.009$ 90% CL. In the following,

we shall use the CCFR limits to elucidate the constraints imposed on the theory. As mentioned earlier, theories with manifest left-right symmetry are constrained by our measurement. Using the limit on $|\eta|$, limits on the ζ -vs- ϵ plane are presented in Fig.B3.

We have so far explicitly assumed that the incident neutrino is left handed. We point out that the ν_μ and $\bar{\nu}_\mu$ events surviving the cuts of this analysis are predominantly from K^+/K^- decays. Whereas the limits on neutrino polarization from π -decay are stringent (< 0.0041), the limits on neutrino polarization from K -decay are less precise (< 0.064).[B6] Thus, the incident neutrino could have a right handed component (with mass, $m_{\nu_R} < m_K - m_\mu = 388$ MeV) at about 5% level. The CCFR measurement on $|\eta|^2$ then restricts the mass of the right handed W-boson, assuming $m_{\nu_R} < 388$ MeV, to:

$$\begin{aligned} M_{W_R} &< (5.1 \times M_{W_L}) \text{ for } \zeta \rightarrow 0 \\ \zeta &< (2.2^0) \text{ for } M_{W_R} \rightarrow \infty. \end{aligned} \tag{11}$$

Precision measurements in μ -decay and nuclear β -decay experiments (for details see Ref.B2) constrain regions in $\zeta - \epsilon$ plane. These limits, however, apply to the special case when the right handed neutrino (corresponding to $SU(2)_R$) is light. Limits from the neutrino experiments are independent of this assumption.

Lorentz Structure from the Inverse Muon Decay: The inverse muon decay process (IMD), although statistically less precise, provides an independent and unique information upon the Lorentz structure of the weak current. Being a purely leptonic interaction its theoretical predictions are unambiguous. The recent high statistics measurements by the CCFR and CHARM II collaborations provide considerable improvement over the past measurements. The absolute cross section of

the IMD process, as measured by the CCFR collaboration, is:[B7]

$$\sigma(IMD) = [16.93 \pm 0.94(\text{stat.}+\text{syst.})] \times E_\nu \times 10^{-42} \text{cm}^2 \text{ [CCFR]} \quad (12)$$

It agrees well with the theoretical prediction (for $s \gg m_\mu^2$): $\sigma(\nu_\mu + e \rightarrow \mu + \nu_e) = 17.2 \times 10^{-42} E_\nu(\text{GeV})\text{cm}^2$. This agreement of the measured and the predicted rates enable us to limit the allowed region at 90% CL in the neutrino polarization (P: =-1 for left handed neutrino; =+1 for right handed neutrino) vs current admixture parameter ($\lambda = +1$ for $V - A$; =-1 for $V + A$) plane (Figure B4), which complements the limits from the μ -decay and those extracted from the ν_μ and $\bar{\nu}_\mu$ differential cross sections.

Conclusion and Future Prospects: The recent precision measurements in the neutrino sector have considerably extended the previous sensitivities in searching for a deviation from the expected Lorentz structure of the weak current. The CCFR limit on $|\eta|^2 = |g_R/g_L|^2 < 0.0015$ (90% CL) complements the μ -decay measurements and, being independent of the mass of the right handed neutrino, extends the limit. The measurement of total cross section of the IMD process has reached an accuracy comparable to the measurement of inclusive ν -N total cross section, and provides a powerful constraint on the scalar coupling of leptons which is inaccessible to μ -decay experiments. Efforts are underway for mounting a next generation deep inelastic neutrino experiment at the Fermilab Tevatron with a large intensity Main injector and new Linac.[B8] Such an experiment, with a cumulative statistics of 20×10^6 CC events, after all cuts, should provide a fertile ground for precision measurements of structure functions and electroweak parameters, and offer a unique venue to search for the “missing” parity conserving component of weak interactions.

Acknowledgement: I thank my gracious hosts at the Moriond Conference. I wish to express my gratitude to Mrs. Norry for her kindness and help while I lay ill at Les Arc. I acknowledge the dedicated efforts of the Fermi National Accelerator Laboratory staff and of many individuals at our home institutions. This research was supported by the National Science Foundation and the Department of Energy.

Reference

- [A1] M.A. Kozhushner & E.P. Shabalin, Soviet Physics JETP **14**, 676(1962).
- [A2] W. Czyz *et al.*, Nuovo Cimento **34**, 404(1964).
- [A3] M.S. Marinov *et al.*, Sov.Jour.Nucl.Phys. **3,4**, 437(1966).
- [A4] K. Fujikawa, Ann. of Phys. **68**, 102(1971).
- [A5] R.W.Brown and J.Smith, Phys.Rev. **D3**, 207(1971).
- [A6] J. Lovseth and M. Radomski, Phys. Rev. **D3**, 2686(1971).
- [A7] R.W. Brown *et al.*, Phys. Rev. **D6**, 3273(1972).
- [A8] K. Fujikawa, Phys. Rev. **D8**, 1623(1973).
- [A9] R. Belusevic and J. Smith, Phys. Rev. **D37**, 2419(1988).
- [A10] S.R.Mishra, "Rare Processes in ν -N Interactions", review talk presented at Neutrino '88, Boston. Proceedings of The 13th. International Conference on Neutrino Physics and Astrophysics, edt.J.Schneps *et al.*, World Scientific, Boston(1988) pp.259.
- [A11] A.E. Asratyan *et al.*, Sov.Jour.Nucl.Phys., **25,5**, 558(1977).
- [A12] F.W.Busser *et al.*, "Recent results from the CHARM experiment", Proc.Conf.Neutrino'81, Hawaii, 328(1981); ed. V.Peterson; published by HEP group, Dept. of Phys., University of Hawaii.
- [A13] F.Bergsma *et al.*, Phys. Lett., **122,2**, 185(1983).
- [A14] B.A.Schumm *et al.*, Proc. of XXIII Recontre de Moriond, Electroweak Interaction & Unified theories, Les Arc, Savoie, France, Mar.(1988),pp.413-420.
- [A15] G.Geiregat *et al.*, Phys.Lett., **B245**, 271(1990).

- [A16] R.C.Allen *et al.*, Phys.Rev.Lett., **64**, 1330(1990).
- [A17] The relevant energy is the non-muonic energy associated with the event at the vertex region. For details of the calibration see W.K.Sakumoto *et al.*, Nucl.Inst.Meth., **A294**, 179(1990), and B.A.Schumm, Ph.D. thesis, University of Chicago, 1989, & P.Z. Quintas, Ph.D. thesis, Nevis labs, Columbia University, 1991; also S.R.Mishra *et al.*, Phys.Rev.Lett., **63**, 132(1989); S.R.Mishra *et al.*, Phys.Lett., **B252**, 170(1990).
- [A18] We have published results on the charm-induced opposite sign dimuons with $E_{\mu 2} \geq 9$ GeV cut: C.Foudas *et al.*, Phys. Rev. Lett., **64**, 1207(1990); and with $E_{\mu 2} \geq 5$ GeV cut: M.Shaevitz, invited review talk presented at Neutrino'90, CERN, Geneva, Jun(1990), to be published.
- [A19] P.Marage *et al.*, Z.Phys. **C43**, 523(1989).
- [A20] The contribution to our entire dimuon sample, from diffractively produced vector mesons, other than J/ψ , and their subsequent decay into muon pairs, is negligible ($< .2$ events); for the neutrino production of J/ψ we used a calculation by, V.Barger *et al.*, Phys.Lett., **B92**, 179(1982). The estimated J/ψ contribution to dimuons with $E_{HAD} \leq 1$ GeV was less than 3 events, centered about the mass 3.1 GeV.
- [A21] R.Hofstadter and H.R.Collard, in Landolt-Bornstein, "Numerical Data and Functional Relationship in Science and Technology", Springer-Verlag, Berlin, 1967, Vol.I/2, p.26.
- [A22] M.G.Olsson *et al.*, Phys.Rev., **D17**, 2938(1978).
- [A23] In the neutrino-nucleon trident production calculation, we included the Pauli suppression operative at small momentum transfers.
- [B1] M.B.A. Beg *et al.*, Phys. Rev. Lett., **38**, 1252(1977); M.Gell-Mann, P.Ramond, R.Slansky, Rev. Mod. Phys., **50**, 721(1978).

- [B2] M.Strovink, Proc. of Leptonic Session of XXI Rencontr de Moriond, Les Arc, March (1986), Ed. J. Tran Thanh Van, pp.209. Also see, A.Jodido et al., Phys. Rev. D34, 1967(1986).
- [B3] CDHS Collab.: H. Abramowicz et al., Z.Phys. C12, 225(1982)
- [B4] CCFR Collab.: S.R.Mishra et al., Nevis Preprint # 1428, May(90); submitted to Phys.Rev.Lett.
- [B5] S.R.Mishra and F.Sciulli, Phys. Lett., B244, 341(1990). Slac measurements could be found in, S. Dasu et al., Phys. Rev. Lett., 61, 1061(1988). For the details of the empirical parametrization of the SLAC data see L.W. Whitlow, Ph.D. thesis, SLAC-357, Mar(1990).
- [B6] Review of Particle Properties, Phys. Lett., B 204, 1988. For π -decay see page 167; for K-decay see page 180.
- [B7] CCFR Collab.: S.R. Mishra et al., Phys.Rev.Lett., 63, 132(1989); Phys.Lett., B252, 170(1990). CHARM II Collab. D.Geiregat et al., CERN-EP/90-76, Jun(90); submitted to Phys.Lett.B.
- [B8] S.R.Mishra in Proc. of "Physics at Fermilab in the 1990's", Breckenridge, Colorado, Aug (1989). Ed. D.Green and H.Lubati, World Scientific, Singapore. Also see, M.Shaevitz in these proceedings, and S.R.Mishra (Nevis Preprint # 1426) in Proc. of "Workshop on Hadron Structure Functions and Parton Distribution" at Fermilab, Batavia, Ill., Apr.(1990); to be published.

Table 1: A1: Trident Analysis: Extraction of trident signal for three different $E_{\mu 2}$ cuts: 4.5, 5, and 9 GeV. Whereas the 4.5 and 5 GeV cut employ muon range in the target, the '9 GeV' cut requires the spectrometer reconstruction of the non-leading muon.

$E_{\mu 2}$ cut	$\geq 4.5\text{GeV}$	$\geq 5.0\text{GeV}$	$\geq 9.0\text{GeV}$
$(E_{HAD} \leq 1 \text{ GeV}) + (M_{\mu\mu} \leq 2 \text{ GeV})$	22	20	12
$(2 \leq E_{HAD} \leq 52 \text{ GeV}) + (M_{\mu\mu} \leq 2 \text{ GeV})$	1527	1330	578
$(E_{HAD} \leq 1 \text{ GeV}) + (M_{\mu\mu} > 2 \text{ GeV})$	8	6	3
$(2 \leq E_{HAD} \leq 52 \text{ GeV}) + (M_{\mu\mu} > 2 \text{ GeV})$	1908	1691	959
Signal	15.5	15.3	10.2
Geometric & Kinematic corrections	2.39	2.52	3.69
Fully Corrected Tridents	37.0	38.5	37.6
(error)	(12.4)	(12.3)	(13.3)

Table 1: B1: Systematic Errors on $|\eta|^2$: Estimates of systematic errors on $|\eta|^2$ as determined by the CCFR collaboration.

Sources	$\pm \delta \eta ^2$
Radiative correction	0.00004
Relative flux ($\pm 2\%$)	0.00017
R	0.00020

Figure Caption

Figure A1: Feynman diagram showing the neutrino trident production in ν_μ - A scattering via the W and the Z channels.

Figure A2: Invariant mass distribution of observed muon pairs $M_{\mu\mu}$ (solid symbols), and neutrino trident Monte Carlo calculation (histogram) normalized to the data (8532 events).

Figure A3: Measured E_{HAD} distribution of the dimuon data with $M_{\mu\mu} \leq 2$ GeV (circles), compared with the measured E_{HAD} distribution of the dimuon data with $M_{\mu\mu} > 2$ GeV (crosses). The trident signal appears in the lowest hadron energy bin.

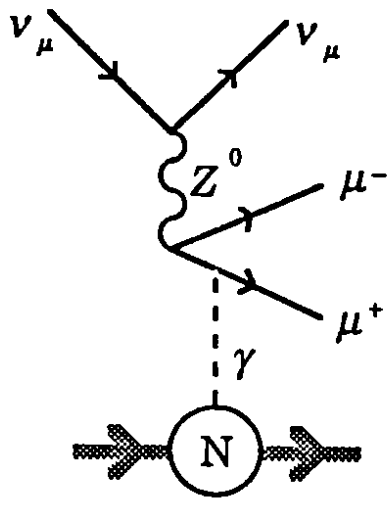
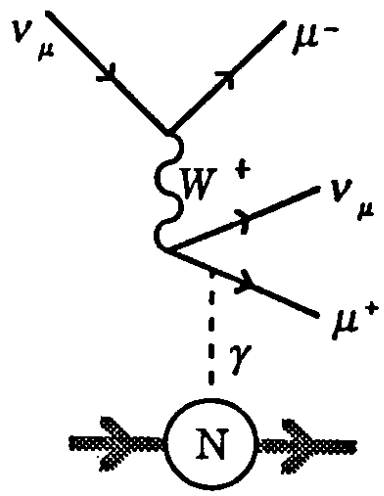
Figure A4: E_{HAD} distribution of the dimuon data with (a) $2 < M_{\mu\mu} \leq 3$ GeV (in solid circles), and (b) $3 < M_{\mu\mu} \leq 5$ GeV (in squares). The inset shows a hadronic dimuon Monte Carlo simulation of E_{HAD} distribution with $0 < M_{\mu\mu} \leq 2$ GeV, compared to those with $2 < M_{\mu\mu} \leq 5$ GeV.

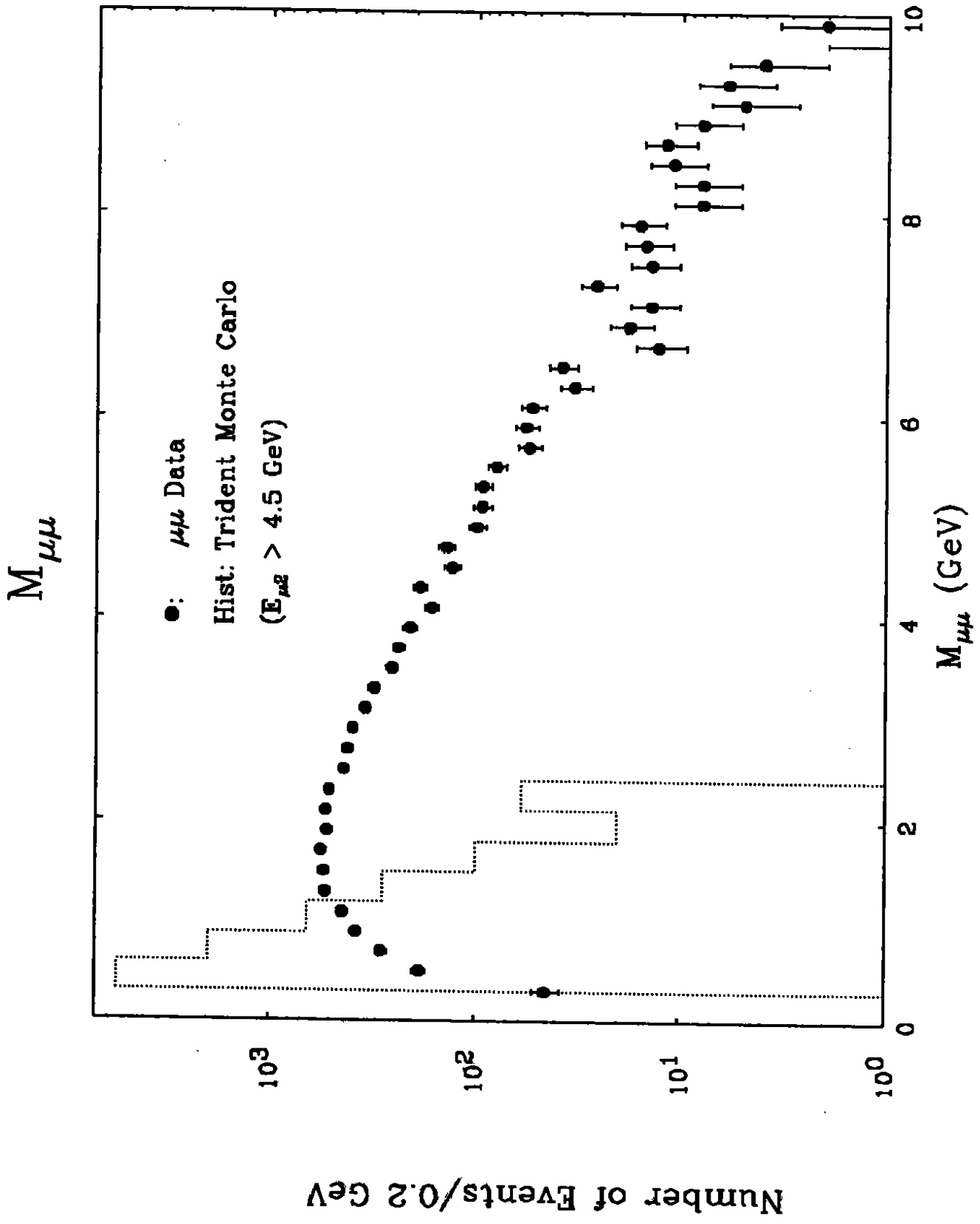
Figure B1: Distribution of the variable $y = \frac{E_{HAD}}{E_\nu}$, for (a) ν_μ - and (b) $\bar{\nu}_\mu$ -induced charged current events (CCFR data) after imposing cuts on muon momentum and hadron energy. The Monte Carlo prediction is shown as histograms.

Figure B2: $\bar{q}(x, Q^2)$ as a function of Q^2 (GeV^2) in various x -bins (CCFR data). Notice that $\bar{q}(x, Q^2)$ is consistent with zero for $x > 0.45$.

Figure B3: Limits on ζ - ϵ plane from neutrino experiments. These limits are independent of the mass of the right handed neutrino.

Figure B4: Limits on neutrino polarization and current admixture (P - λ) plane from IMD measurements by the CCFR collaboration (90% CL).





[Fig.A2]

ν Tridents

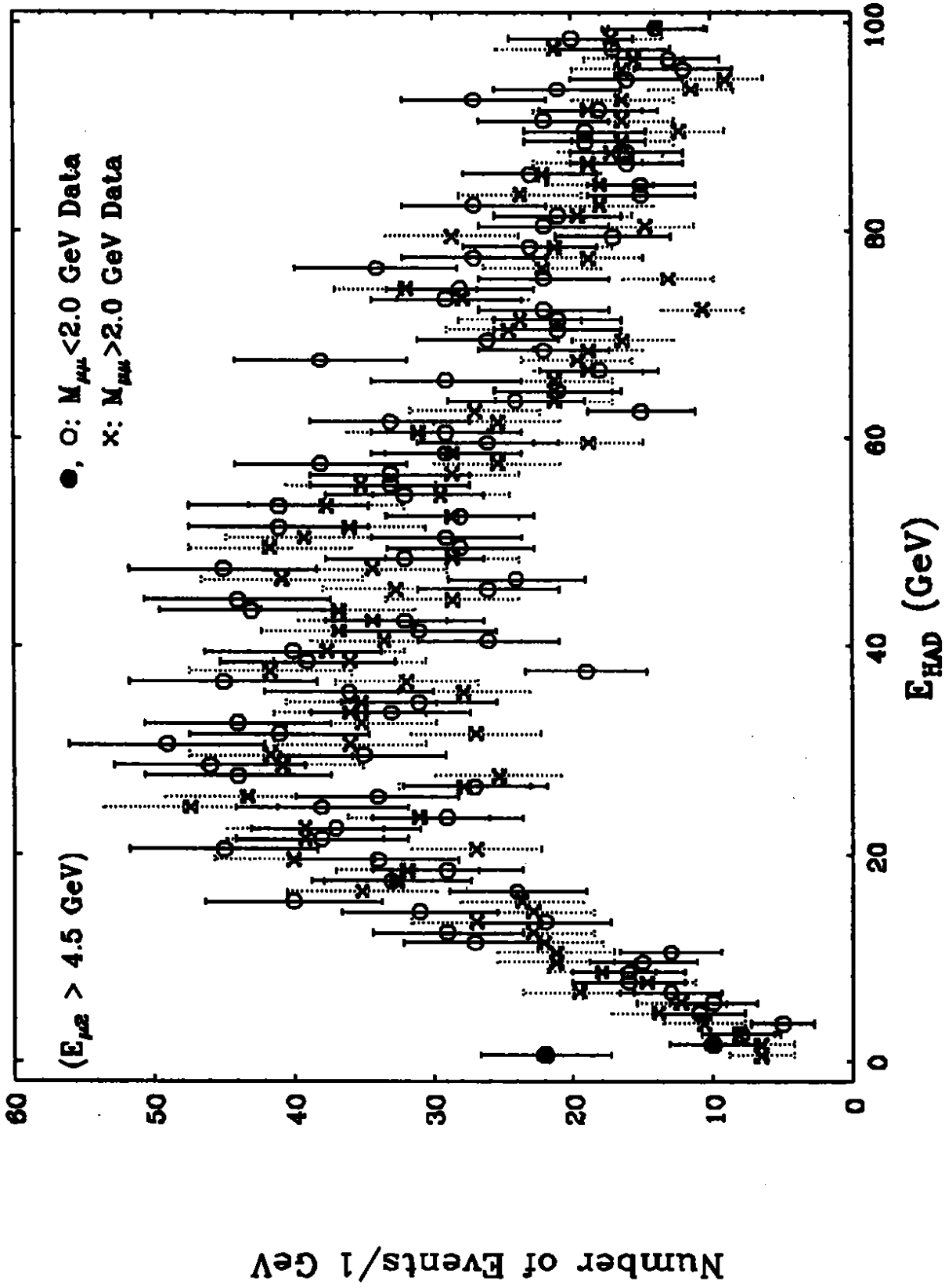


[Fig.A3]

$E_{HAD}: 2.0 < M_{\mu\mu} < 3.0 \text{ GeV} \ \& \ 3.0 < M_{\mu\mu} < 5.0 \text{ GeV}$

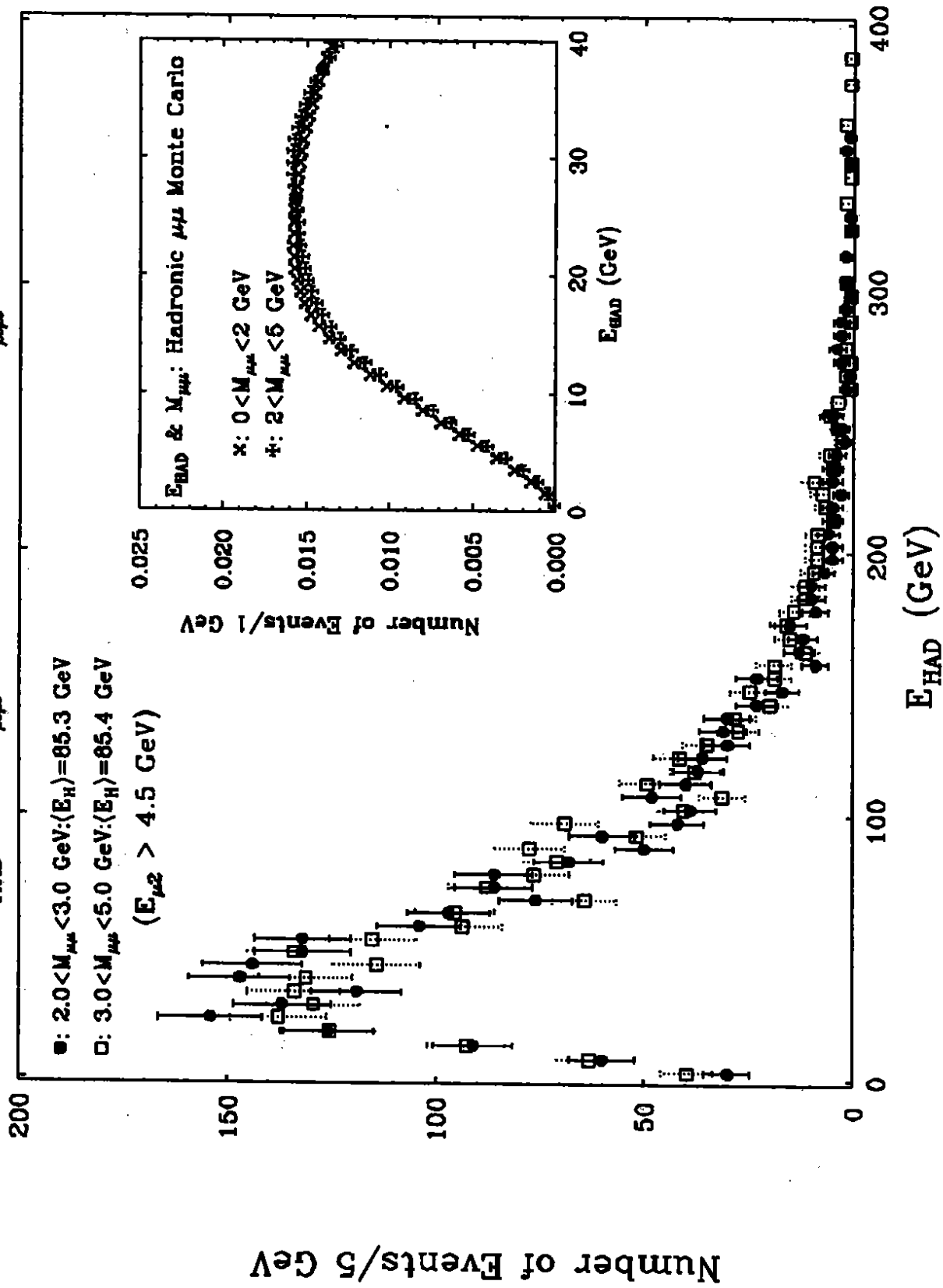


[Fig.A4]

$\nu_\mu: y = E_{HAD}/E_\nu$ (CCFR Data)

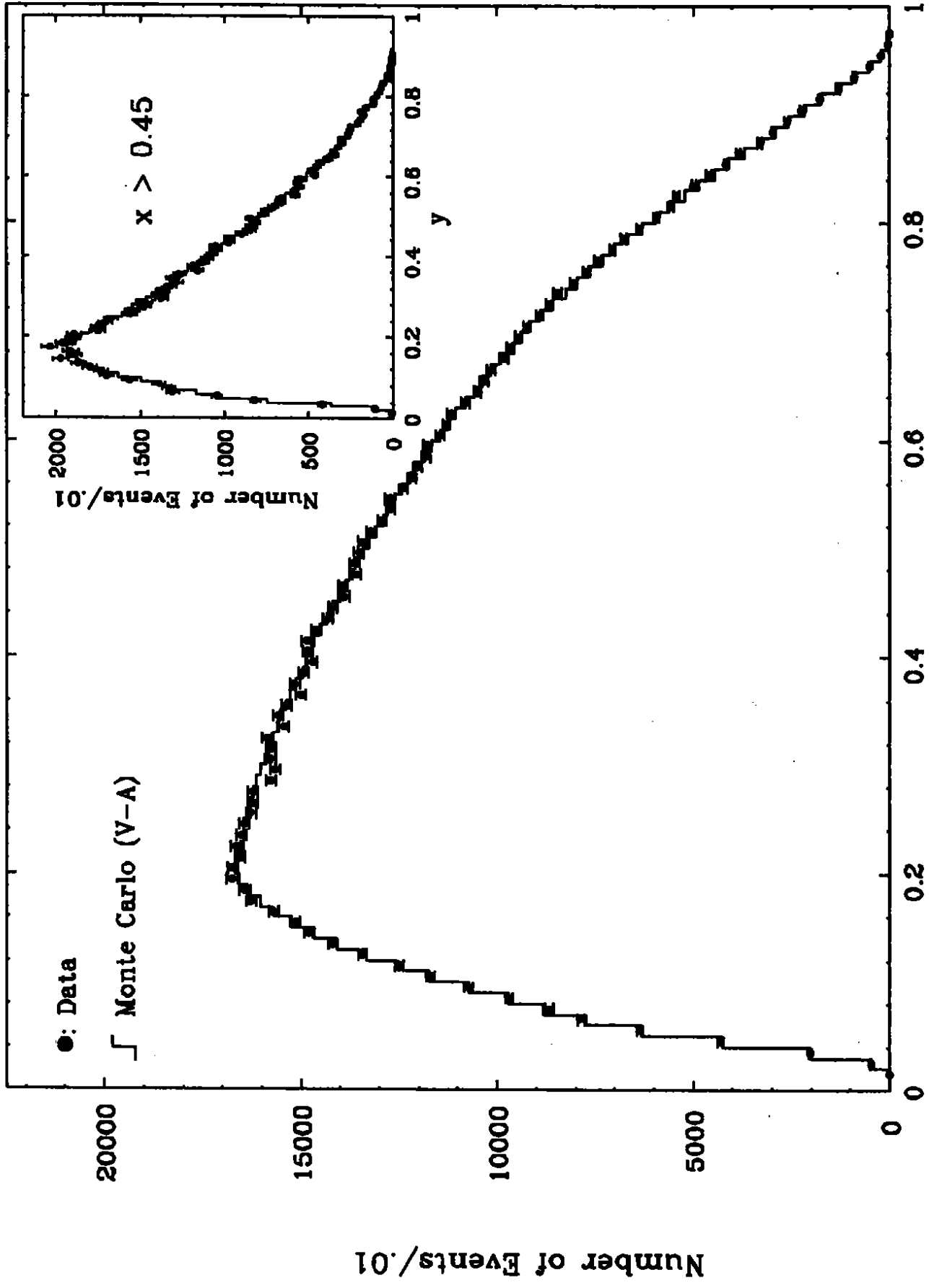


(Fig. B1a)

$\bar{\nu}_\mu: y = E_{HAD}/E_\nu$ (CCFR Data)

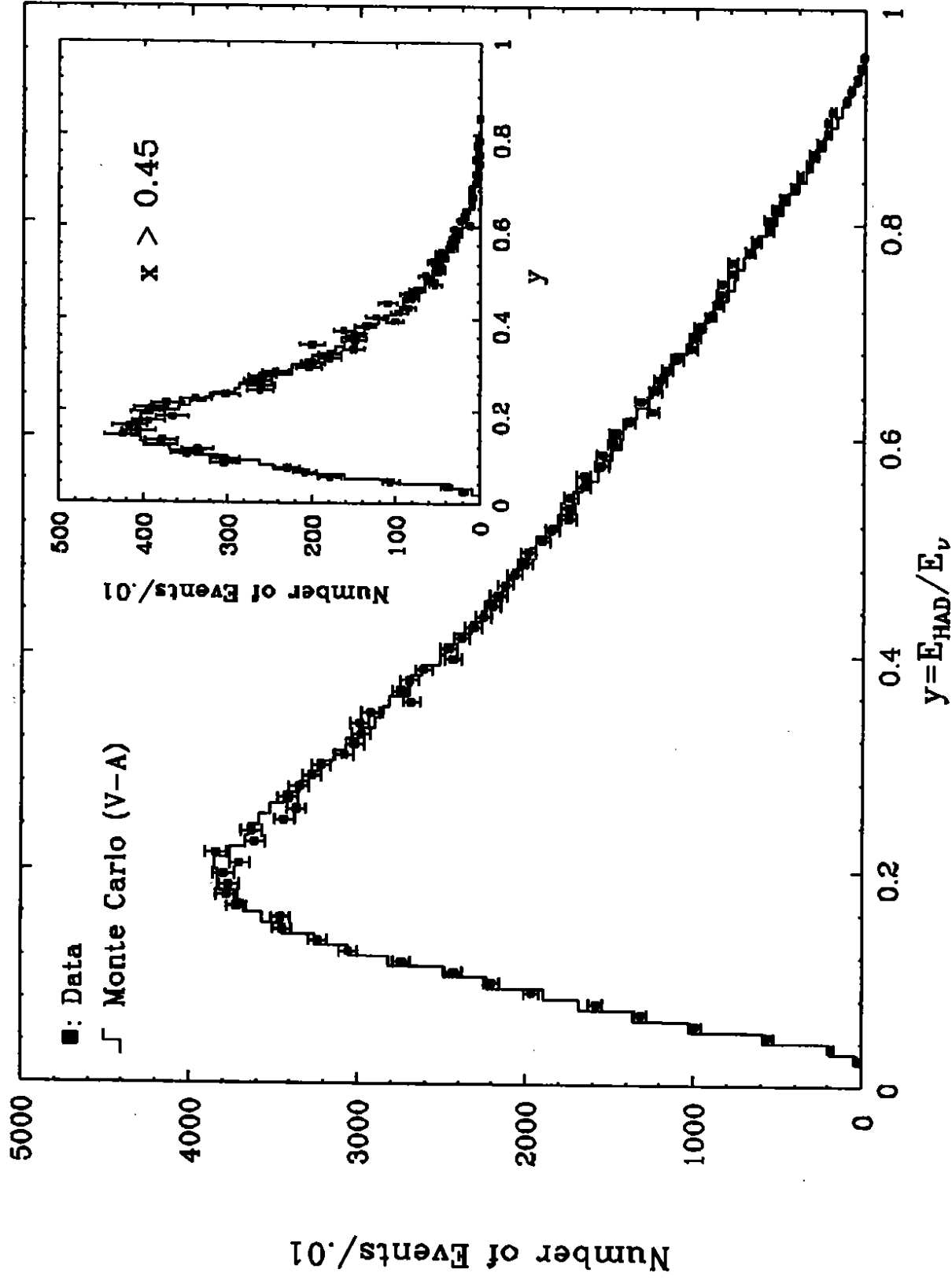
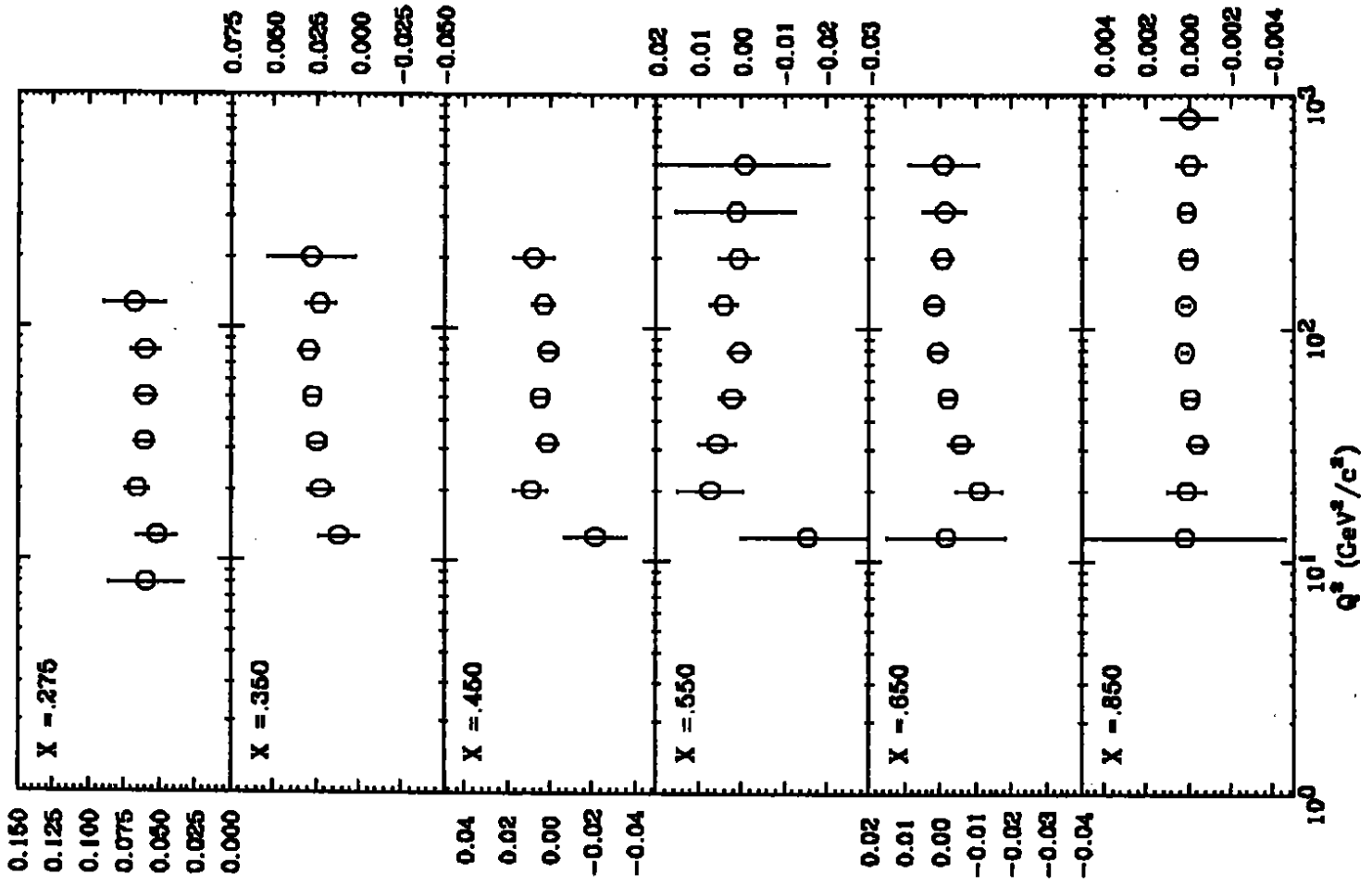
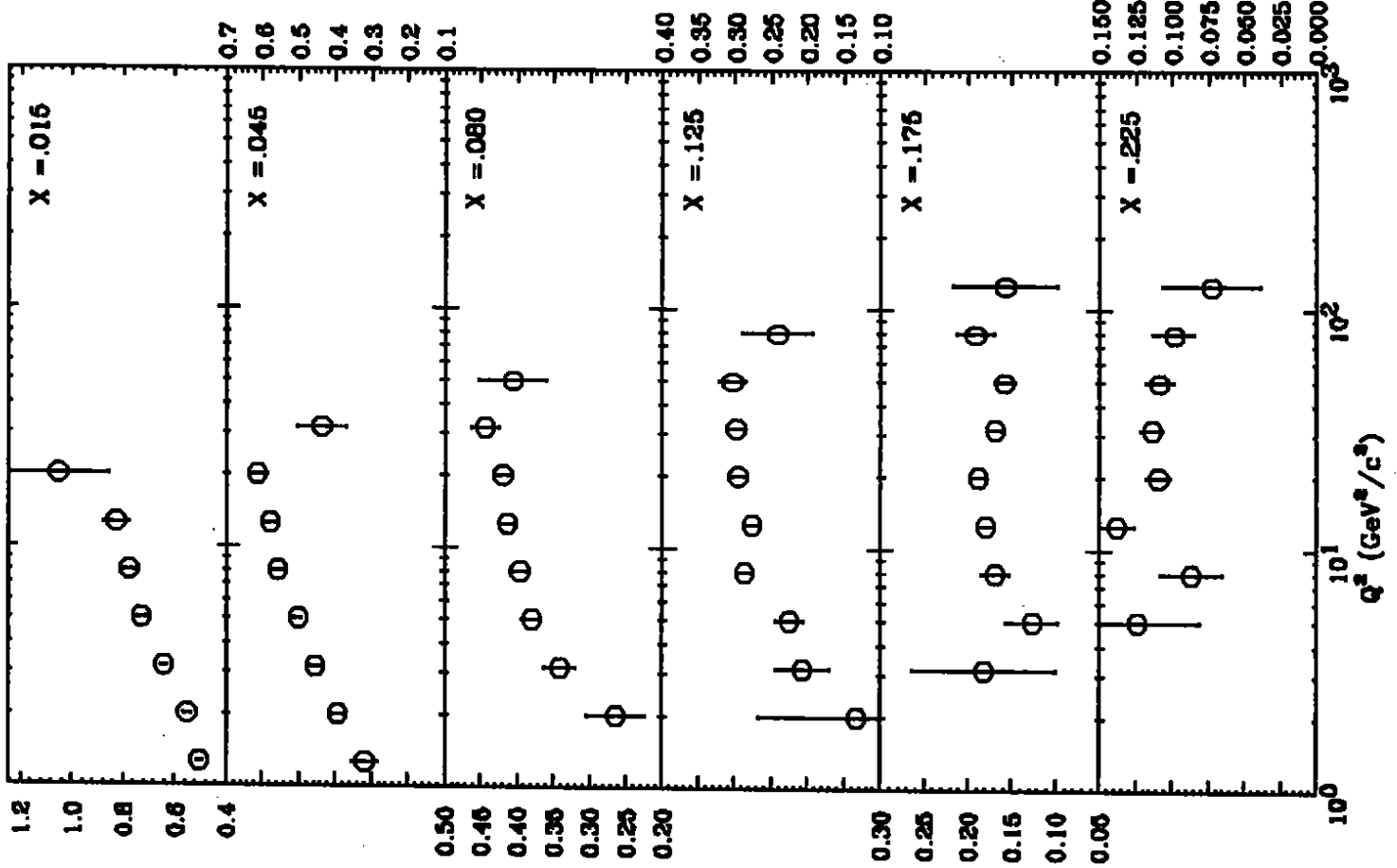
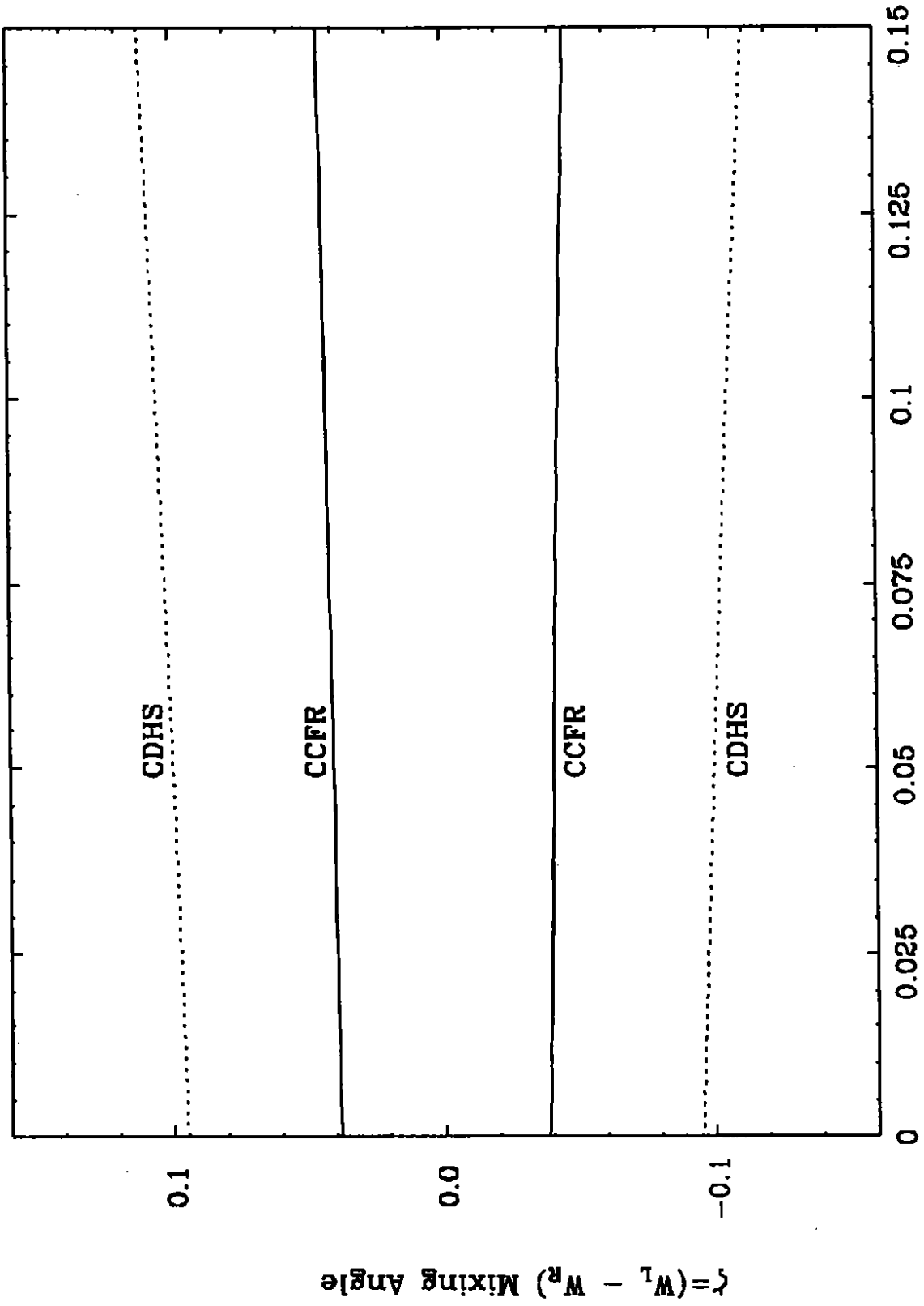


(Fig. B1b)

$xq(x)$: CCFR (QTB): $50 \leq E_\nu < 600$ GeV (Fig. B2)



Limits in ζ - ϵ Plane



$$\epsilon = M^2(w_1) / M^2(w_2)$$

(Fig. B3)

Limits in P- λ Plane

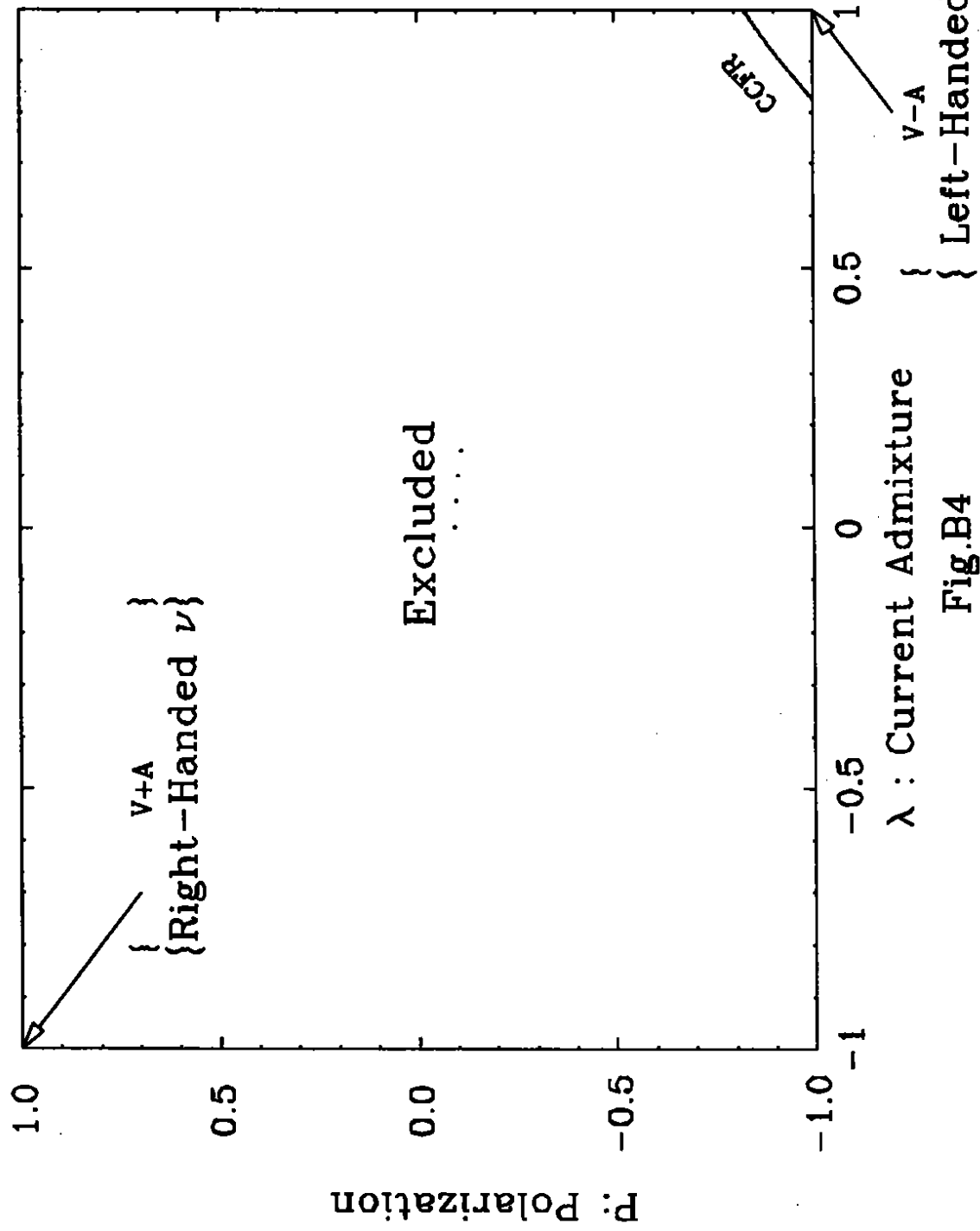


Fig.B4